

CHARACTERISTICS OF COCHLEAR NUCLEUS ONSET UNITS STUDIED WITH A MODEL

Sridhar Kalluri^{1,2} and Bertrand Delgutte^{1,2,3}

¹*Harvard-MIT Division of Health Sciences and Technology*
243 Charles Street, Massachusetts Eye and Ear Infirmary
Boston, MA 02114, USA

²*Eaton-Peabody Laboratory*
Massachusetts Eye and Ear Infirmary

³*Research Laboratory of Electronics*
Massachusetts Institute of Technology

1. Introduction

Onset neurons are characterized by their preferential response to onset transients in acoustic signals. These neurons have long been of interest to auditory scientists because of the importance of onset transients for the perception of speech and music, as well as for sound localization and stream segregation [6][43][48].

Onset units are found throughout the central auditory system, beginning with the ventral cochlear nucleus (VCN) [17]. VCN onset units are particularly interesting from a modeling perspective because their response properties differ sharply from those of their auditory-nerve (AN) inputs. Intracellular labeling of physiologically characterized cells shows that VCN onset units form a heterogeneous group in that they are morphologically associated with several anatomical classes, including stellate cells, bushy cells and octopus cells [31][34][40][41]. Given this heterogeneity, it is not surprising that current knowledge of the neuronal characteristics associated with onset unit responses is still very much incomplete. In particular, there is no universally accepted scheme for classifying onset units into subtypes based on their response properties nor for associating physiological subtypes with anatomical cell types [5][13][35][36]. A long-term goal of our research is to determine the neuronal properties underlying the responses of different subtypes of onset units to acoustic stimulation and thereby clarify the correspondence between cell types and physiological subtypes of onset units. As a first step towards that goal, this chapter describes a mathematical model used to identify a minimum set of neuronal characteristics required to obtain key response properties common to all VCN onset units.

Two types of models have been used for investigating the underlying mechanisms of onset unit response patterns. One approach has been to construct a detailed biophysical model, including active membrane channels [38], and electro-anatomical characteristics of the cell body and dendritic tree [7][25]. Such models point to the importance of fast membrane dynamics and weakly excitatory synapses requiring coincidence of many inputs to obtain onset response patterns to tonal signals. However, at present there is insufficient information pertaining to ion channels and synaptic distributions in most VCN neurons to adequately constrain these biophysical models. A further difficulty is that different parameters would be required for each of the different cell types that give rise to onset response proper-

ties. Because of the drawbacks associated with detailed biophysical models, we have developed a very general phenomenological model that contains the essential elements without attempting to model detailed biophysical properties specific to a given neuronal class.

Previous phenomenological models of onset units [2][9] have suggested the need for a high-pass filtering mechanism such as depolarization block, threshold accommodation, or receptor desensitization that would decrease the probability of discharge during sustained depolarization. However, these models only examined in detail the neuronal responses to a limited set of stimuli. We extend the results of these earlier models by investigating a relatively large set of stimuli and neuronal response characteristics. A major result of our study is that three separate response properties are identified that strongly constrain the model. If these properties are correctly predicted then the model is successful in predicting responses to a broader range of stimuli. This chapter focuses on these three crucial, physiological properties:

- (1) The onset peri-stimulus time (PST) histogram for high-frequency tone bursts consisting of a prominent peak followed by little or no response during the on-going part of the stimulus [32]. This property contrasts with the sustained response patterns of auditory-nerve inputs.
- (2) Entrainment of spike discharges to low-frequency (< 1 kHz) tones [35] (i.e., the occurrence of one spike on every cycle of the stimulus). AN-fibers rarely entrain, in that multiple tone cycles typically occur between successive spikes.
- (3) Similar thresholds for broadband noise and characteristic frequency (CF) tones [46]. Again, this property contrasts with that of AN fibers, where CF tone thresholds are always significantly lower than noise thresholds.

Our model of a VCN onset cell is based on an integrate-to-threshold point neuron whose inputs are AN fibers acting via excitatory synapses. We use a two-part strategy for identifying model characteristics necessary for obtaining realistic onset response properties. First, the dynamic properties of the cell membrane are fit to intracellular measurements of voltage responses to current injections in octopus cells (which are the cells most convincingly associated with VCN onset-responding neurons [31][34][40]). Second, synaptic and input properties of the model (specifically synaptic strength, number of independent AN inputs, and CF distribution of these inputs) are constrained by the three response properties enumerated above.

2. Methods

2.1 Model of Auditory-Nerve Fibers

AN-fiber responses were computed using a model that simulates the primary features of temporal discharge patterns for tones and noise [8]. The model includes the following features.

- (1) The bandpass tuning of an AN fiber is modeled as a linear gammatone filter [18].
- (2) A second-order, low-pass filter with a 1.1 kHz cutoff frequency models the reduction of synchronization to high-frequency tones.
- (3) Adaptation is described using a model of the inner-hair-cell synapse [45].
- (4) To describe the statistical properties of discharge patterns, the spike train is modeled as a non-stationary renewal process whose instantaneous probability of discharge is the product of a component representing excitatory drive from the hair cells and a component

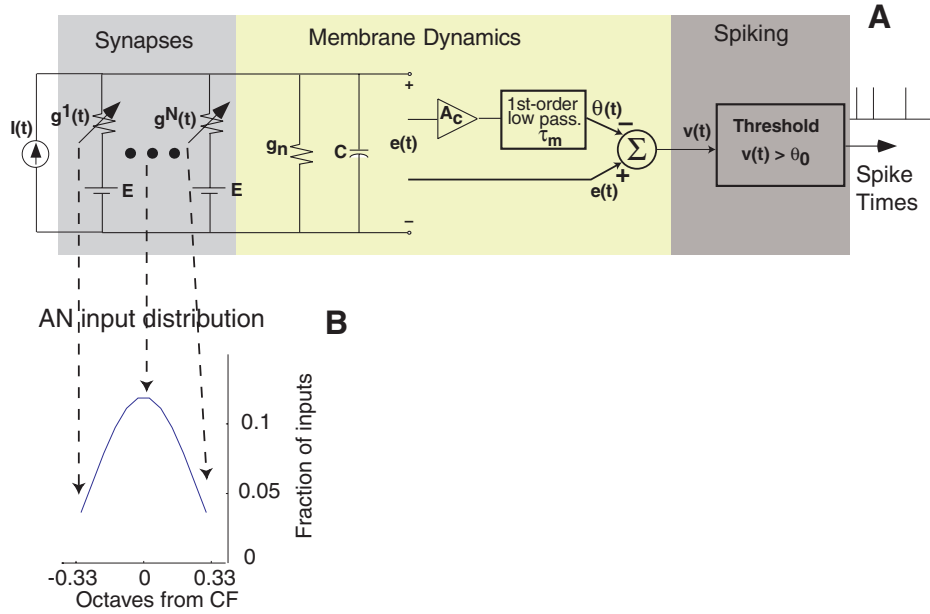


Figure 1 The model for an onset responding neuron. A. Schematic of the integrate-to-threshold point-neuron model. B. The distribution of characteristic frequencies (CFs) of auditory nerve (AN) inputs to the model neuron. In this case the total CF range of the AN inputs is 2/3 of an octave.

representing refractory properties of the fiber [19]. Spikes for each AN fiber are produced using a set of independent random number generators.

2.2 Point-Neuron Model of VCN Onset Cells

Figure 1A illustrates a schematic representation of the model onset neuron. The model is deterministic. We divide it into two components, input and membrane dynamics. All of the model parameters are listed in Table 1.

2.2.1 Input

The model contains only excitatory synapses that are driven by spikes from AN fibers. A spike causes a smooth transient increase in conductance of the corresponding synapse. The duration of the conductance change is 500 microseconds for all synapses. Synaptic strength (or magnitude of conductance change) is the same for all synapses. For illustrative purposes synaptic strength is normalized to the unitary synaptic strength (defined as the threshold strength of a synapse such that an isolated input spike gives rise to an output spike).

The number of independent AN inputs to the model neuron is also a parameter. We examine values of this parameter between 1 and 128. The distribution of CFs of the AN inputs is described by a Gaussian-like density function (Figure 1B). The function is symmetric about the CF of the model onset unit on a log-frequency axis. In all figures, the CF of the model onset unit is 6 kHz. The total frequency range spanned by the inputs is a parameter of the model.

Table 1. Summary of model parameters. Asterisk denotes that the parameter is varied in some illustrations.

Membrane parameters	
Membrane time constant: $\tau_m = C/g_n$	0.39 ms
Accommodation time constant: τ_θ	0.67 ms
Accommodation gain: A_c	0.49
Absolute refractory period	0.75 ms
Synaptic and input parameters	
Normalized synaptic strength	0.16*
Number of AN inputs	100*
CF range of AN inputs	2/3 octave*
Duration of synaptic conductance change	0.5 ms

2.2.2 Membrane Dynamics and Refractoriness

The dynamic properties of the membrane are based on the two-factor model for membrane electrical excitability first investigated by Hill and others [16][29][33]. In the model (Figure 1A), the membrane voltage $v(t)$ is the difference between an integrative factor $e(t)$ and an accommodation factor, $\theta(t)$. The integrative factor results from low-pass filtering (temporally integrating) the summed synaptic inputs. The time constant of the integrative factor, τ_m , is very short (< 1 ms), and is determined by the membrane capacitance. The accommodation factor is itself a low-pass filtered version of the integrative factor. Since $\theta(t)$ is subtracted from $e(t)$, it effectively acts as a high-pass filter that emphasizes transients in the synaptic inputs. The time constant, τ_θ , of the accommodation factor is longer than that of the integrative factor, but is still very short. The accommodation factor results in a decrease in membrane voltage during sustained depolarization. An accommodation gain, A_c , controls the amount of accommodation relative to the integrative factor.

The neuron produces a spike discharge whenever the membrane voltage exceeds a fixed threshold, θ_0 . For a fixed refractory period following a spike, the neuron cannot fire, and both the integrative process and the accommodation process are undefined. Thus, no attempt is made to model the spike waveform. At the end of the refractory period, the integrative process is reset to zero, while the accommodation process resumes the value it had prior to the spike.

3. Results

3.1 Membrane Electrical Properties

Our model for membrane electrical excitability is based on properties of octopus cells derived from *in vitro* experiments. We chose octopus cells because they are the most convincingly identified onset responders in the VCN [13][31][34][40]. Parameters of the membrane model were estimated using voltage responses of octopus cells to current injections.¹

Only responses of the octopus cell to depolarizing current injections were used for estimating parameters. Figure 2 shows responses of an octopus cell to step current injections of

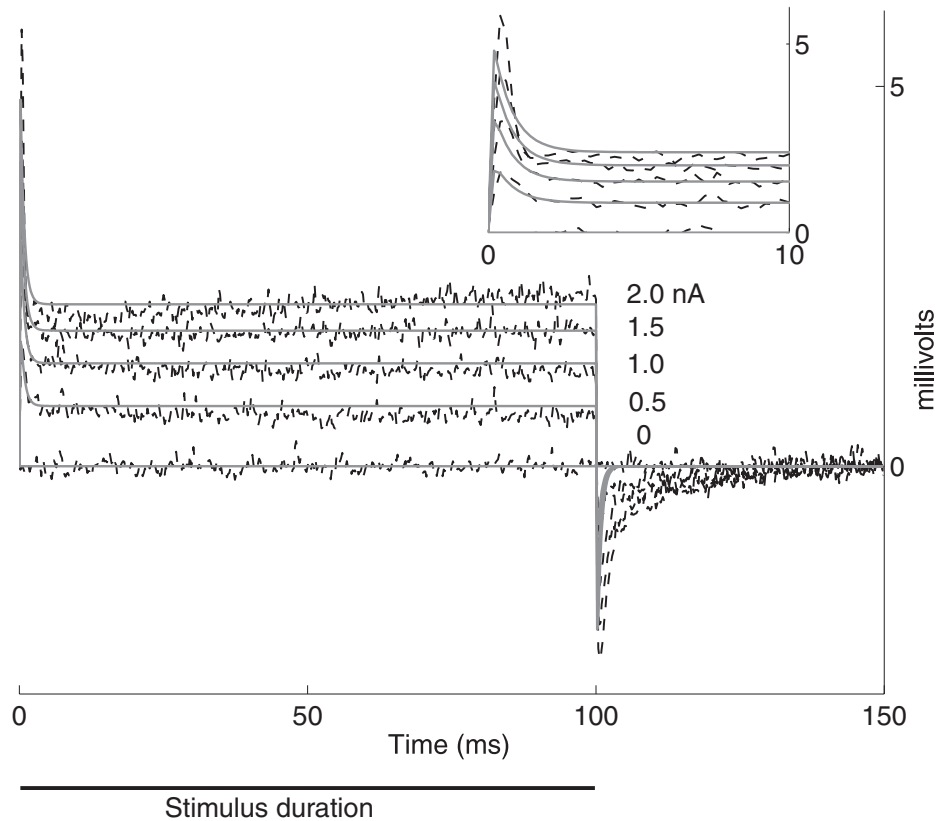


Figure 2 Model and octopus cell responses to step current injections. Solid curves represent the model and dashed curves indicate the octopus cell responses [14]. Inset shows the first 10 ms of the response.

different amplitudes and model responses that best fit the data according to a least-squares-error criterion [14].

The sub-threshold octopus cell response exhibits a rapid rise and a slower decline to a constant steady-state level in the first 10 ms after the onset of the stimulus. A model with a single dynamic process (i.e., with a single time constant) can fit either the rise or the fall of the octopus cell response, but not both. At least two dynamic processes (i.e., with two time constants) are required to concurrently capture both properties of the response. Figure 2 shows that our model successfully captures the main features of the octopus cell response; the best-fit parameters are $\tau_m = 0.25$ ms, $\tau_\theta = 0.64$ ms, and $A_c = 0.62$. The two dynamic processes, membrane integration and accommodation, confer a very brief maximum in membrane voltage for positive current injections that is reflected in the single spike elicited at onset by supra-threshold current steps in the model and in octopus cells (not shown). The model predicts spikes at the offset of large negative current injections; such spikes are also observed in octopus cells.

There are some systematic deviations between model and data evident in the responses to large current injections. In particular, the model underestimates the height of the initial peak in the response and the rapidity of the early decline of the response (inset of Figure 2). At

least one additional time constant in the accommodation factor is required to accurately describe these properties of the octopus cell response.

We estimated model parameters using responses of five different octopus cells to current injections. The residual variance of the best-fit model was always less than 7% of the total variance of the data. The model parameters were similar across these five cells. In the following sections are described the model's response to acoustic signals using the median parameter values for the membrane model listed in Table 1.

3.2 *Synaptic Strength and Number of Independent AN Inputs*

We examined, in the model, the effect of synaptic strength and the number of independent AN inputs on temporal discharge patterns in response to tone-burst stimulation. More specifically, we looked at how the gross shape of the PST histogram associated with CF-tone responses and the synchronization and entrainment to a low-frequency tone (600 Hz) vary with these model parameters.

3.2.1 PST Histograms for Tones

A defining property of VCN onset units is the shape of their PST histograms of high-frequency tone burst responses. These histograms have a prominent peak at stimulus onset, followed by a low discharge rate during the steady-state portion of the stimulus over a wide range of stimulus levels [4][5][13][35][46]. Figure 3 illustrates how PST histograms of CF tone burst responses at 20 dB above threshold depend on synaptic strength and on the number of independent AN inputs to a model neuron.

As a reference, a PST histogram is shown for a 6-kHz (CF) tone burst response of an AN input (Figure 3D), which has a sustained response with fast adaptation. The model response has different PST histogram shapes depending on the number of inputs and synaptic strength (Figure 3A, 3B, 3E, 3F). When the model exhibits weak synapses and many (100) independent AN inputs, its PST histogram has an onset shape with no sustained activity (Figure 3A). Increasing the synaptic strength moderately (Figure 3E) produces a PST histogram of the model response that is more sustained, similar to the PST histogram of the AN input. When the strength of synapses is moderate, but the number of AN inputs is reduced, the PST histogram of the response is still of the onset variety, but with more sustained activity (Figure 3B). Figure 3C shows how the shape of PST histograms varies as a function of synaptic strength and the number of independent AN inputs. We identify three types of model responses (criteria shown in the caption of Figure 3):

- (1) a region where there is little or no response,
- (2) a region where the PST histogram has an onset shape, and
- (3) a region where the PST histogram has a sustained shape.

Although the shape of the PST histogram depends on both the number of independent AN inputs and on synaptic strength, the latter is more important. In order to obtain the onset form of PST histogram associated with high-frequency tone bursts, the synaptic strength must be weak.

Spontaneous rate depends in a similar way on synaptic strength and the number of independent AN inputs (with synaptic strength being more important). The model has a spontaneous rate magnitude (< 2 spikes/s) appropriate for an onset unit when the synaptic strength is weak. These observations are similar to those associated with previous models of onset neurons [23] [38].

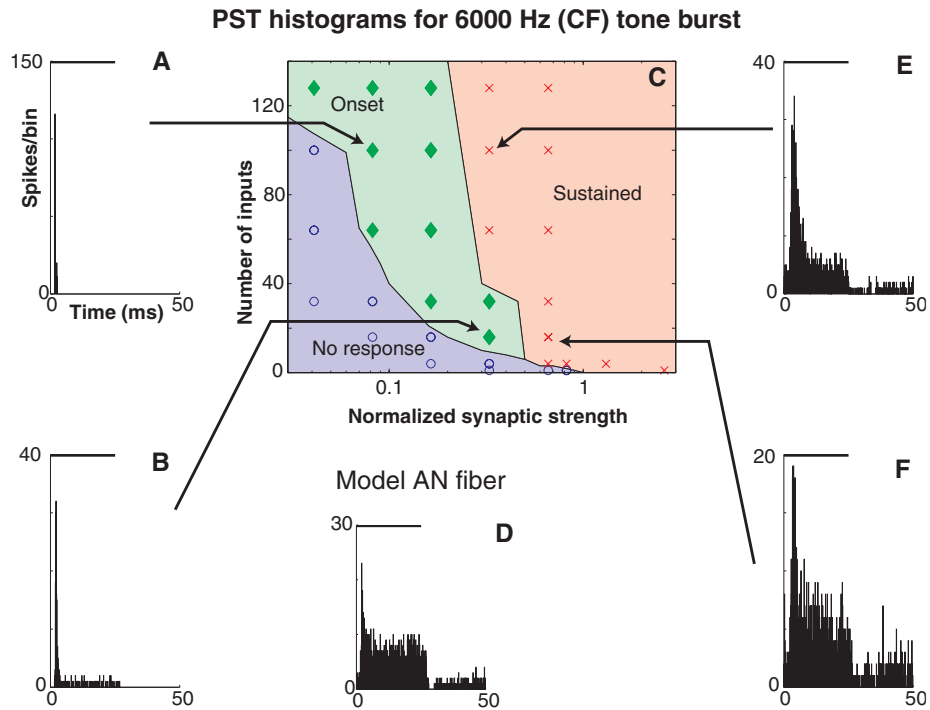


Figure 3 PST histograms of high-frequency, CF tone burst responses as a function of synaptic strength and number of independent AN inputs. A, B, E, and F: PST histograms of model responses for a synaptic strength and number of independent AN inputs indicated by arrows. Synaptic strength is indicated by arrows (250 stimuli, bin width = 0.1 ms). D: PST histogram of a 6-kHz (CF) tone burst response (50 dB SPL) of a model AN fiber (250 stimuli, bin width = 0.1 ms). Bars above the histograms indicate duration of the stimulus. C: Variation of the shape of PST histograms of high-frequency CF tone responses with a variable number of inputs and synaptic strength. Criterion for classifying onset PST histograms was the same as used by Winter and Palmer [46] — the ratio of onset rate to steady-state rate must be greater than 10, and the steady-state rate must be less than 50 spikes/s. It is assumed that the cell is unresponsive to CF tonal stimuli when the threshold is greater than 70 dB SPL.

3.2.2 Phase-Locking to Low-Frequency Tones

VCN onset units phase-lock to low-frequency tones (< 1 kHz) with greater precision than most other VCN units; their synchronization to such signals is also greater than that of AN fibers [13][35]. These units also entrain to low-frequency tones below 1 kHz (i.e., they discharge on every cycle of the tone). Entrainment is a singular property that is rarely (if ever) observed in other types of VCN units. Our analysis shows how entrainment to a 600-Hz tone burst (presented at 90 dB SPL) depends on synaptic strength and the number of independent AN inputs associated with a model neuron (Figure 4).

For reference, an interspike-interval histogram and a period histogram of an AN fiber are shown in Figure 4B. These histograms are similar to those observed in actual AN fibers. Figure 4A shows interval and period histograms for the model when it has 100 inputs and the synapses are weak. The period histogram shows that the response is highly synchronized to the stimulus. The single peak in the interval histogram at a duration associated with a single stimulus period (1.7 ms) indicates that the response is entrained to the stimulus. There is a

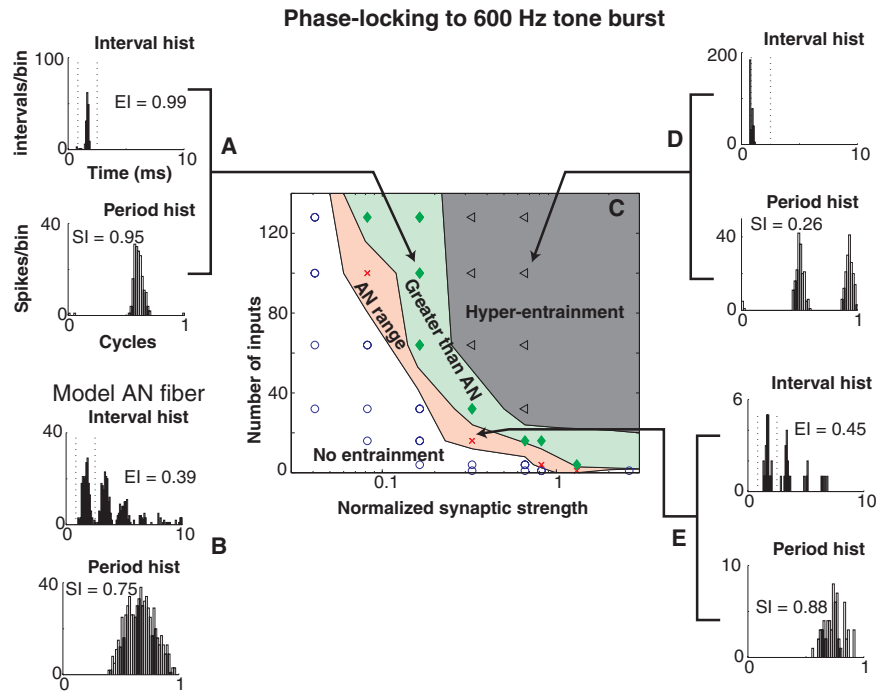


Figure 4 Entrainment of the model neuron (CF = 6 kHz) to a 90 dB SPL, 600-Hz tone as a function of synaptic strength and number of independent AN inputs. A, D, and E: Interval histograms (20 stimuli, bin width = 0.1 ms) and period histograms (64 bins) of the model with the number of inputs and synaptic strength indicated by arrows. B: Interval histogram (200 stimuli, bin width = 0.1 ms) and period histogram (64 bins) for the response of a model AN fiber (CF = 6 kHz). C: Variation of entrainment index (EI) with synaptic strength and number of inputs. EI is the ratio of the number of intervals with a duration equal to a stimulus period divided by the total number of intervals. The different symbols and shading delineate four separate regions according to qualitative differences in entrainment: i) No entrainment (EI = 0), ii) range for model AN inputs ($0 < EI < 0.78$), iii) greater than model AN inputs ($EI > 0.78$), and iv) hyper-entrainment (more than one spike per cycle).

qualitative change in response characteristics when the synaptic strength is increased (Figure 4D). The presence of two separate peaks in the period histogram indicates that the response has multiple spikes in a stimulus period (i.e., hyper-entrainment). When both the synaptic strength and the number of inputs are low, entrainment in the model is similar to entrainment observed in the AN inputs (Figure 4E).

Figure 4C illustrates how entrainment varies in the model as a function of the synaptic strength and the number of independent AN inputs. The parameter space is divided into four regions according to how well the model response entrains to the tone (quantified by the entrainment index [EI], defined in the caption of Figure 4):

- (1) no entrainment,
- (2) entrainment in the range of the AN model ($0 < EI < 0.78$),
- (3) entrainment greater than the AN model, which is the range we expect to be appropriate for onset units ($EI > 0.78$), and
- (4) hyper-entrainment (multiple spikes per cycle of the stimulus).

Entrainment occurs within the onset range when there are either few inputs with a high synaptic strength or there are many weak AN inputs. Synchronization to low-frequency

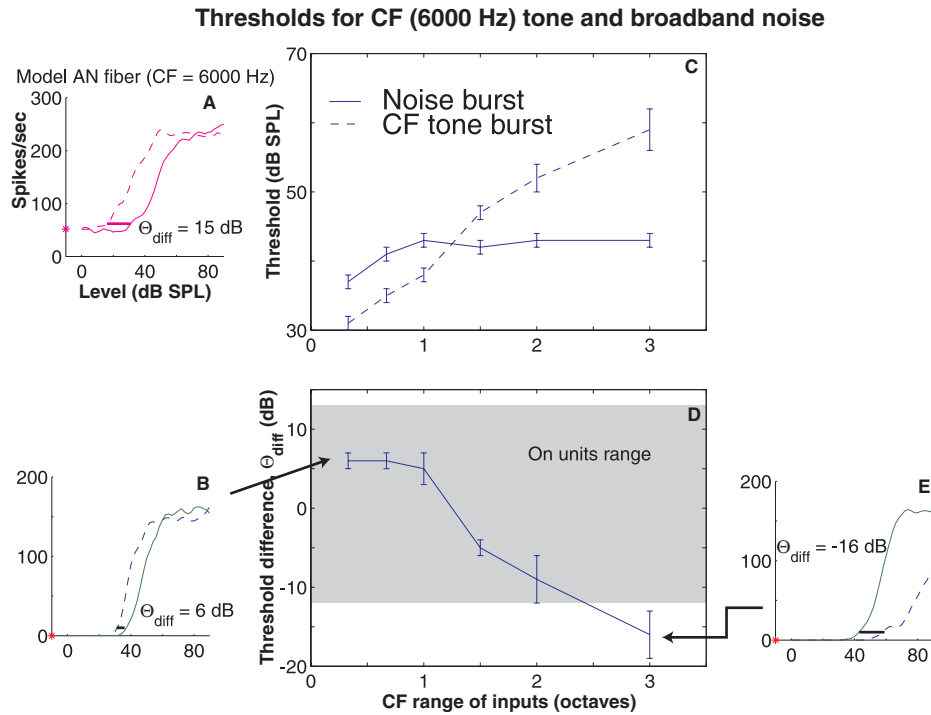


Figure 5 Broadband noise (bandwidth = 20 kHz) threshold and 6-kHz (CF) tone threshold as a function of CF range of inputs. A. Rate versus level for broadband noise (solid) and CF tone (dashed) for a model AN fiber. Horizontal bars show difference between broadband noise threshold and CF-tone threshold. B and E. Same as in the model for the CF range of inputs indicated by arrow. C. Broadband noise threshold and CF tone threshold as a function of CF range of inputs. D. Difference between broadband noise threshold and CF tone threshold (Θ_{diff}) as a function of CF range of inputs. Shaded area is the range for Θ_{diff} in onset units with CFs near 6 kHz [46].

tones and the standard deviation of first-spike latency in high-frequency tone-burst responses also show similar, but more weakly constrained dependence on synaptic strength and the number of inputs.

Taken together, the results of Figures 3 and 4 show that the model must have relatively weak synapses and many independent AN inputs (> 32) in order to exhibit both onset PST histograms for high-frequency tones and entrainment to low-frequency tones. In this parameter range, the model also has a spontaneous rate, a standard deviation of first-spike latency and synchronization indices characteristic of onset units. In the following figures, the number of inputs is 100 and the synaptic strength is 0.16. These values correspond to the region of the parameter space (Figure 3C and 4C) where the model exhibits temporal response characteristics typical of onset units.

3.3 CF Distribution of AN Inputs

Winter and Palmer [46] have found that the threshold for broadband noise (in dB SPL) exceeds the CF-tone threshold by more than 15 dB in AN fibers and VCN chopper units but is less than 15 dB among onset units. They propose that this particular response property can be accounted for by assuming that onset units integrate their inputs across a broader frequency range than do other VCN units or AN fibers. Their proposal is based on the difference

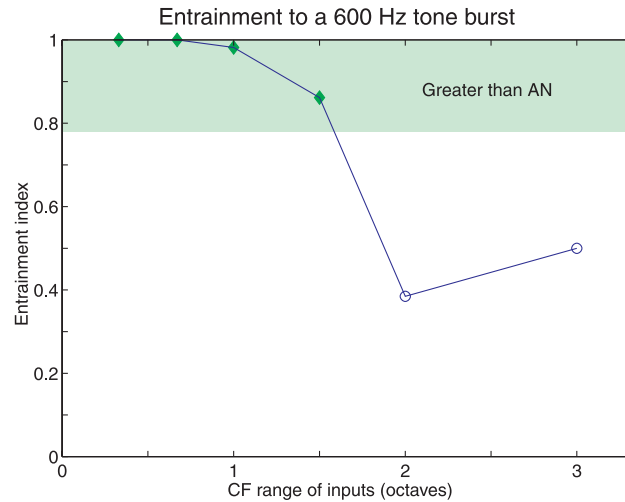


Figure 6 Entrainment to a 600-Hz tone as a function of the CF range of AN inputs for a model cell with a CF of 6 kHz. The EI decreases with an increasing CF range of inputs. Shaded region ($EI > 0.78$) indicates an entrainment greater than occurs in model AN fibers and corresponds to the similarly labeled region in Figure 4.

between broadband noise energy and CF-tone energy integrated by a linear broadband filter being less than the energy difference for a linear narrow band filter. We examined whether a broad CF range of AN inputs to the model is required in order to obtain a difference in threshold between broadband noise and CF tones in the range observed in onset units.

Figure 5 shows how the CF range of AN inputs in the model affects thresholds for broadband noise and CF tones. Serving as a reference point, Figure 5A shows rate versus level curves for broadband noise and CF tones associated with an AN input from the model. The rate-level curve for noise is shifted to higher stimulus levels relative to the rate-level curve for tones. The difference in threshold between the tone and noise is 15 dB. Figure 5B shows rate-level curves for the model when the CF range of AN inputs is 1/3 octave. Although the curve for noise is displaced toward higher stimulus levels relative to the curve for tones (as occurs in the AN model), the threshold difference is only 6 dB. Figure 5E shows rate-level curves for the model when the CF range of AN inputs is 3 octaves. In this case the rate-level curve for noise is shifted toward lower stimulus levels relative to the rate-level curve for tones. The threshold for noise is actually 16 dB less than the threshold for tones.

Figure 5D shows that the difference between the broadband noise threshold and the CF-tone threshold decreases monotonically as the CF range of the AN inputs increases from 1/3 octave to 3 octaves. Figure 5C shows the noise thresholds and the tone thresholds used to compute the threshold differences. The threshold difference decreases as the CF range of AN inputs increases because the noise threshold varies less than the tone threshold. These observations follow from the properties associated with the fast membrane dynamics as well as from the large number of AN inputs acting via weak synapses that make the model response dependent on coincident spikes on the inputs. The model responds more readily when there are spikes associated with several inputs as compared to when there are only a few inputs. The noise threshold does not vary much because the number of AN inputs responding to the stimulus stays relatively constant as the CF range of inputs increases from 1/3 octave to 3 octaves. On the other hand, the tone threshold varies substantially because the number of

inputs that respond to the stimulus varies greatly as the CF range of inputs increases. When the CF range of AN inputs is small, a tone evokes a large response in many of the model inputs, thus leading to a low threshold. When the CF range of AN inputs is broad, only a few model inputs respond to the tone, thus leading to a high threshold.

For all of the CF ranges of AN inputs examined, the model produced onset PST histograms and low spontaneous rates. However, the fine-time structure of the discharge pattern associated with low-frequency (entrainment and synchronization) and high-frequency tone bursts (standard deviation of first-spike latency) varied as a function of the CF range of AN inputs. Of these response properties, entrainment to low-frequency tones was the most sensitive to the CF range of AN inputs.

Figure 6 shows that entrainment to a 90-dB SPL, 600-Hz tone decreases as the CF range of AN inputs increases in the model. A major reason why entrainment decreases is that AN fibers with different CFs have different response latencies introduced by the cochlear traveling wave. Therefore, there is an increasing degree of desynchronization of spikes across the tonotopically organized array of AN fibers as the CF range of inputs increases. Because the model is highly sensitive to temporal coincidence of spikes from the array of AN fibers, this desynchronization causes entrainment in the model to diminish.

These results show that the fine-time structure of discharge patterns, as well as the thresholds associated with broadband noise and CF tones, constrain the CF range of AN inputs to the model. The shaded regions of Figure 5D and Figure 6 indicate the range of threshold difference and entrainment, respectively, for VCN onset units. In the model unit, the CF range of AN inputs needs to be less than 1.5 octaves for both the threshold difference and the entrainment to be within the range observed for onset units.

4. Discussion

In this chapter, we have identified a minimum set of properties required for obtaining onset discharge patterns in response to acoustic stimulation. Specifically, we have determined constraints on the nature of the AN inputs and associated synapses such that the model exhibits responses characteristic of VCN onset units. Although several parameters affect each of the onset response properties, some are especially important. A weak synaptic strength is the most important determinant of an onset PST histogram for high-frequency tone bursts. This finding is consistent with results from previous models of VCN bushy cells and octopus cells [23][24][38]. We also have found that entrainment to low-frequency tones is jointly determined by synaptic strength, number of inputs and the range of CFs spanned by the inputs. In order to simultaneously produce onset PST histograms for high-frequency tone bursts and entrainment to low-frequency tones, the model must have weak synapses and many independent AN inputs (> 32) whose CFs span less than 1.5 octaves. The difference between broadband noise threshold and CF tone threshold also depends greatly on the CF range of AN inputs. Together, the threshold differential and entrainment constrain the CF range of AN inputs to be at most 1.5 octaves in our model.

Model parameters that produce realistic onset responses are generally consistent with the anatomical data. Specifically, the constraint of a large number of AN inputs giving rise to weak synapses is consistent with anatomical observations from octopus cells and other labeled onset responders that these cells have a large number of synapses, all of which are small relative to the size of the cell [15][27][31][41]. On the other hand, the model predicts that the CF range of inputs needs to be limited to 1.5 octaves, a property in apparent conflict with the view that onset units receive AN inputs from a very wide CF range. This view is

based on the observation that dendrites of octopus cells and other labeled onset units are oriented perpendicularly to iso-frequency bands of incoming AN fibers and therefore must span a wide range of CFs [15][22][41]. However, for a CF of 6 kHz, our 1.5 octave limit corresponds to a substantial length (20%) of the basilar membrane according to the Liberman cochlear frequency map for the cat [26]. Since the CF distribution of onset units is biased toward high frequencies [46], this 20% of the basilar membrane length might actually represent an even more substantial proportion of the relevant array of AN inputs to the onset cell population. A more rigorous test of our model prediction would require quantification of the length of the basilar membrane innervated by AN inputs to labeled onset neurons.

Previous model-based investigations have focused on onset responses to sinusoidal signals. Synaptic strength was found to be the principal factor determining PST histogram shape in response to high-frequency tone bursts in models of octopus and bushy cells [23][24][38][39]. Rothman and Young [39] have further shown that convergence of many independent AN inputs is required for their model of VCN bushy cells to exhibit the exquisite synchronization to low-frequency tones observed in onset units. Our findings are consistent with these observations but show that entrainment imposes an even more powerful constraint on the model. Evans [9] has shown, using a phenomenological model, that fast membrane excitability and threshold accommodation together provide more faithful onset PST histograms and a better match to the threshold differential between tonal and noise stimuli than either property alone. Our own model results are in accord with those of Evans and further show that the CF range of inputs is an important factor as well. Our results extend the findings of previous studies by considering the model properties required to simultaneously explain several onset-response properties. Specifically, we find that onset PST histograms for high-frequency tone bursts, entrainment to low-frequency tones and the threshold difference between broadband noise and CF tones are particularly informative measures for constraining model parameters when considered together as a group.

In this chapter, we have shown how model responses depend on properties of AN inputs and associated synapses for fixed membrane properties obtained by fitting the membrane model to octopus cell responses to current injections. It is known that membrane electrical properties differ among cells in the VCN [11][15][30][47]. Electrical properties may vary across the heterogeneous onset population of neurons as well. Certain properties of the model response patterns (e.g., the detailed features of PST histograms) vary with changes in the cell's membrane characteristics. However, the key response properties examined in this chapter do not change significantly as long as parameters of the membrane model remain within certain limits. Specifically, our conclusions regarding inputs and synapses remain valid as long as the time constant of membrane excitability is small (< 1 ms) [20][21]. Furthermore, in order to produce both onset PST histograms in response to high-frequency tone bursts and entrainment to low-frequency tones, the model must have a strong and relatively rapid accommodative threshold.

Although accommodation is a phenomenological concept, it could be instantiated by incorporating voltage-gated ion channels into the model. Specifically, at least two kinds of channels may be necessary to include. The transient maximum in membrane voltage observed upon stimulation by a depolarizing, sub-threshold step current can be implemented using an outward-rectifying ion channel that is active at voltages slightly above the resting potential. The low-threshold potassium channel that is blocked by 4-aminopyridine is such a channel. It is found in VCN bushy and octopus cells [12][15][28]. Accommodation, in the form used in our model, also causes a transient decrease in membrane voltage at the onset of

negative current steps and a transient peak in the membrane voltage at their offsets (as well as spikes for sufficiently negative-going current injections). These aspects of the response to negative current steps are also observed in octopus cells. Channels that rectify inward at voltage levels below the resting potential can be used for implementing these membrane properties. The hyperpolarization-activated channel that is blocked by Cs^+ (a.k.a. I_h) and found in principal cells of the medial nucleus of the trapezoid body and octopus cells of the VCN [3][15] possesses such characteristics. A model for the octopus cell that includes the sorts of channels described has been implemented; its responses to step-current injections are qualitatively similar to data recorded from octopus cells [7].

Accommodation might also be implemented using other mechanisms, such as desensitization of synaptic receptors [44]. Although receptor desensitization may not be required to account for octopus-cell-response properties (because membrane voltage shows accommodation in the absence of synaptic inputs [12][15]), it may play a role in other onset responding classes of neurons.

When onset units were first studied, recurrent inhibition was proposed as a possible mechanism for producing the onset-discharge pattern of response to tone bursts [13]. This particular hypothesis lost much of its appeal as a consequence of intracellular recordings from onset units failing to manifest sustained hyperpolarization in response to tonal stimulation [37]. Recent work with iontophoretic injection of inhibitory transmitter antagonists [10] has provided evidence that inhibition plays a role in shaping the response properties of a subclass of onset units. Despite this recent evidence we have not included inhibitory inputs in our model because too little is known about the origin of these inputs to develop a quantitative model and because our primary focus is on response properties common to all types of onset units.

Identifying which neuronal characteristics underlie responses to sound is part of the more general problem of correlating cell structure with function. Understanding such relationships in one class of neurons may help understand its relation in other cell classes. For example we have observed a trade-off between the CF range (and therefore latency spread) of AN inputs and the ability of onset units to entrain to low-frequency tones. Recent evidence suggests that cortical pyramidal cells are similar to VCN onset units in that they act as coincidence detectors [1][42]. Thus, our trade-off may be an instance of a general constraint (with potential counterparts among the pyramidal cells of the cortex) on the ability of neurons to precisely follow successive transients in the stimulus when their inputs are desynchronized.

In this study we have used a phenomenological model, rather than a detailed biophysical model, to identify the characteristics underlying response patterns of onset units. In the context of this book, which examines computational methods for studying audition, it is worth noting our example of a phenomenological model of a neuron that yields useful results pertaining to the mechanisms underlying neuronal signal processing.

5. Conclusions

Using a simple functional model of a VCN cell, we have determined the characteristics required for obtaining onset-response patterns to acoustic stimulation. We find that no single neuronal property confers onset-response characteristics on a VCN neuron. Instead, a combination of properties must be simultaneously present for the model to manifest all response characteristics of onset units. Many independent AN inputs (> 32), weak synapses, fast membrane dynamics, and a high-pass filtering process (such as an accommodative thresh-

old) are all necessary for simulating onset response properties. The CF range of AN inputs further affects the fine temporal structure of discharge as well as the threshold for tones and noise. Together, these effects strongly constrain the entire set of model parameters. Our results suggest three sets of data for characterizing the underlying neuronal features of an onset unit:

- (1) PST histograms of high-frequency tone-burst responses,
- (2) entrainment to low-frequency tones, and
- (3) the differential response threshold of broadband noise and CF tones.

Acknowledgments

Supported by research grant DC02258 and training grant DC00038 from the National Institute on Deafness and Other Communicative Disorders, National Institutes of Health. We thank Stephanie Hequembourg and Craig Atencio for comments on the manuscript.

Note

1. In the original formulation of Hill [16], accommodation was implemented as an increase in the time-varying threshold. Because intracellular recordings from octopus cells show an accommodation of membrane voltage in response to sustained current injections [12][14], we prefer to model accommodation as a change in voltage, $v(t)$, rather than as a change in threshold. Therefore a fixed threshold was used rather than one of a time-varying nature. Because the difference between threshold and membrane voltage determines spiking, the two formulations are mathematically equivalent, but the current formulation is better suited for comparison with intracellular data.

References

- [1] Abeles, M. "Role of the cortical neuron: Integrator or coincidence detector." *Israel J. Med. Sci.*, 18: 83–92, 1982.
- [2] Arle, J. and Kim, D. "Neural modeling of intrinsic and spike discharge properties of cochlear nucleus neurons." *Biol. Cybern.*, 64: 273–283, 1991.
- [3] Banks, M., Pearce, R., and Smith, P. "Hyperpolarization-activated cation current (I_h) in neurons of the medial nucleus of the trapezoid body: Voltage-clamp analysis and enhancement by norepinephrine and cAMP suggest a modulatory mechanism in the auditory brain stem." *J. Neurophysiol.*, 70: 1420–1432, 1993.
- [4] Blackburn, C. and Sachs, M. "Classification of unit types in the anteroventral cochlear nucleus: PST histograms and regularity analysis." *J. Neurophysiol.*, 62: 1303–1329, 1989.
- [5] Bourk, T. *Electrical Responses of Neural Units in the Anteroventral Cochlear Nucleus of the Cat*. Ph. D. Thesis, Massachusetts Institute of Technology, 1976.
- [6] Bregman, A. S. *Auditory Scene Analysis*. Cambridge, MA: MIT Press, 1990.
- [7] Cai, Y., Walsh, E. J., and McGee, J. "Mechanisms of onset responses in octopus cells of the cochlear nucleus: Implications of a model." *J. Neurophysiol.*, 78: 872–883, 1997.
- [8] Carney, L. "A model for the responses of low-frequency auditory-nerve fibers in cat." *J. Acoust. Soc. Am.*, 93: 401–417, 1993.
- [9] Evans, E. F. "Modeling characteristics of Onset-I cells in guinea pig cochlear nucleus." *Proc. NATO Advanced Study Institute on Computational Hearing*, S. Greenberg and M. Slaney (eds.), pp. 1–6, 1998.
- [10] Evans, E. F. and Zhao, W. "Periodicity coding of the fundamental frequency of harmonic complexes: physiological and pharmacological study of onset units in the ventral cochlear nucleus." In *Psychophysical and Physiological Advances in Hearing*, A. R. Palmer, A. Rees, A. Q. Summerfield and R. Meddis, (eds.), London: Whurr Publishers, pp. 186–192, 1998.
- [11] Feng, J., Kuwada, S., Ostapoff, E.-M., Batra, R. and Morest, D. "A physiological and structural study of neuron types in the cochlear nucleus. I. Intracellular responses to acoustic stimulation and current injection." *J. Comp. Neurol.*, 346:1–18, 1994.
- [12] Ferragamo, M. J. and Oertel, D. "Shaping of synaptic responses and action potentials in octopus cells." 21st Midwinter Meeting Assn. Res. Otolaryngol., St. Petersburg Beach, FL, 1998.

- [13] Godfrey, D., Kiang, N., and Norris, B. "Single unit activity in the posteroventral cochlear nucleus." *J. Comp. Neurol.*, 162: 247–268, 1975.
- [14] Golding, N. L., Ferragamo, M. J., and Oertel, D. "Personal communication." 1998.
- [15] Golding, N. L., Robertson, D., and Oertel, D. "Recordings from slices indicate that octopus cells of the cochlear nucleus detect coincident firing of auditory-nerve fibers with temporal precision." *J. Neurosci.*, 15: 3138–3153, 1995.
- [16] Hill, A. V. "Excitation and accommodation in nerve." *Proc. Roy. Soc. (London), Ser. B*, 119: 1936.
- [17] Irvine, D. R. F. *The Auditory Brainstem*. Berlin: Springer-Verlag, 1986.
- [18] Johannesma, P. I. M. "The pre-response stimulus ensemble of neurons in the cochlear nucleus." *Proc. Symp. Hearing Theory*. Eindhoven: IPO, pp. 58–69, 1972.
- [19] Johnson, D. and Swami, A. "The transmission of signals by auditory-nerve fiber discharge patterns." *J. Acoust. Soc. Am.*, 74: 493–501, 1983.
- [20] Kalluri, S. and Delgutte, B. "A general model of spiking neurons applied to onset responders in the cochlear nucleus." Presented at *Computational Neurosciences Conference*, Cambridge, MA, 1996.
- [21] Kalluri, S. and Delgutte, B. "An electrical circuit model for cochlear nucleus onset responders." Presented at *20th Midwinter Meeting of Assoc. Res. Otolaryngol.*, St. Petersburg Beach, FL, 1997.
- [22] Kane, E. C. "Octopus cells in the cochlear nucleus of the cat: Heterotypic synapses upon homeotypic neurons." *Intern. J. Neurosci.*, 5: 251–279, 1973.
- [23] Kipke, D. R. and Levy, K. L. "Sensitivity of the cochlear nucleus octopus cell to synaptic and membrane properties: A modeling study." *J. Acoust. Soc. Am.*, 102: 403–412, 1997.
- [24] Levy, K. and Kipke, D. "Mechanisms of the cochlear nucleus octopus cell's onset response: synaptic effectiveness and threshold." *J. Acoust. Soc. Am.*, 103: 1940–1950, 1998.
- [25] Levy, K. L. and Kipke, D. R. "A computational model of cochlear nucleus octopus cells." *J. Acoust. Soc. Am.*, 102: 391–402, 1997.
- [26] Liberman, M. C. "The cochlear frequency map for the cat: Labeling auditory-nerve fibers of known characteristic frequency." *J. Acoust. Soc. Am.*, 72: 1441–1449, 1982.
- [27] Liberman, M. C. "Central projections of auditory-nerve fibers of differing spontaneous rate. I. Posteroventral and dorsal cochlear nucleus." *J. Comp. Neurol.*, 327: 17–36, 1993.
- [28] Manis, P. and Marx, S. "Outward currents in isolated ventral cochlear nucleus neurons." *J. Neurosci.*, 11: 2865–2880, 1991.
- [29] Monnier, A. *L'Excitation Electrique des Tissus*. Hermann: Paris, 1934.
- [30] Oertel, D., Wu, S. H., Garb, M., and Dizack, C. "Morphology and physiology of cells in slice preparations of the posteroventral cochlear nucleus of mice." *J. Comp. Neurol.*, 295: 136–154, 1990.
- [31] Ostapoff, E.-M., Feng, J., and Morest, D. "A physiological and structural study of neuron types in the cochlear nucleus. II. Neuron types and their structural correlation with response properties." *J. Comp. Neurology*, 346: 19–42, 1994.
- [32] Pfeiffer, R. "Classification of response patterns of spike discharges for units in the cochlear nucleus: Tone-burst stimulation." *Exp. Brain Res.*, 1: 220–235, 1966.
- [33] Rashevsky, N. "Outline of a physico-mathematical theory of excitation and inhibition." *Protoplasma*, 20: 42–56, 1933.
- [34] Rhode, W., Oertel, D., and Smith, P. "Physiological response properties of cells labeled intracellularly with horseradish peroxidase in cat ventral cochlear nucleus." *J. Comp. Neurol.*, 213: 448–463, 1983.
- [35] Rhode, W. and Smith, P. "Encoding of timing and intensity in the ventral cochlear nucleus of the cat." *J. Neurophysiol.*, 56: 261–286, 1986.
- [36] Ritz, L. and Brownell, W. "Single unit analysis of the posteroventral cochlear nucleus of the decerebrate cat." *Neuroscience*, 7: 1995–2010, 1982.
- [37] Romand, R. "Survey of intracellular recording in the cochlear nucleus of the cat." *Brain Res.*, 148: 43–65, 1978.
- [38] Rothman, J., Young, E., and Manis, P. "Convergence of auditory nerve fibers onto bushy cells in the ventral cochlear nucleus: Implications of a computational model." *J. Neurophysiol.*, 70: 2562–2583, 1993.
- [39] Rothman, J. S. and Young, E. D. "Enhancement of neural synchronization in computational models of ventral cochlear nucleus bushy cells." *Aud. Neurosci.*, 2: 47–62, 1996.
- [40] Rouiller, E. and Ryugo, D. "Intracellular marking of physiologically characterized cells in the ventral cochlear nucleus of the cat." *J. Comp. Neurol.*, 225: 167–186, 1984.

- [41] Smith, P. H. and Rhode, W. S. "Structural and functional properties distinguish two types of multipolar cells in the ventral cochlear nucleus." *J. Comp. Neurol.*, 282: 595–616, 1989.
- [42] Softky, W. R. and Koch, C. "The highly irregular firing of cortical cells is inconsistent with temporal integration of random EPSPs." *J. Neurosci.*, 13: 334–350, 1993.
- [43] Stevens, K. N. and Blumstein, S. E. "Invariant cues for place of articulation in stop consonants." *J. Acoust. Soc. Am.*, 64: 1358–1368, 1978.
- [44] Trussell, L. O., Zhang, S., and Raman, I. M. "Desensitization of AMPA receptors upon multi-quantal neurotransmitter release." *Neuron*, 10: 1185–1196, 1993.
- [45] Westerman, L. and Smith, R. "A diffusion model of the transient response of the cochlear inner hair cell synapse." *J. Acoust. Soc. Am.*, 83: 2266–2276, 1988.
- [46] Winter, I. and Palmer, A. "Level dependence of cochlear nucleus onset unit responses and facilitation by second tones or broadband noise." *J. Neurophysiol.*, 73: 141–159, 1995.
- [47] Wu, S. and Oertel, D. "Intracellular injection with horseradish peroxidase of physiologically characterized stellate and bushy cells in slices of mouse anteroventral cochlear nucleus." *J. Neurosci.*, 4, 1577–1588, 1984.
- [48] Zurek, P. M. "The precedence effect." In *Directional Hearing*, W. A. Yost and G. Gourevitch (eds.). New York: Springer-Verlag, 1987.